UNIVERSITY OF CALIFORNIA, SAN DIEGO

Phenotypic manifestations of EIF2AK3 haplotype B genotypes in fibroblasts derived from patients with progressive supranuclear palsy

A Thesis submitted in partial satisfaction

of the requirements for the degree Master of Science

in

Biology

by

David Lenh

Committee in charge:

Professor Shauna Hsiao San Yuan, Chair,
Professor Maho Niwa Rosen, Co-Chair
Professor Eduardo R. Macagno

2017

The Thesis of David Lenh is approved, and it is acceptable in quality and form for publication on microfilm and electronically:

Co-Chair

Chair

University of California, San Diego

2017

DEDICATION

I dedicate this thesis to my family for the unconditional love and support they have provided me during the past twenty-five years of my life. And to my dearest Abrahan Natanael Lara-Pacheco for his guidance, encouragement, and love.

TABLE OF CONTENTS

LIST OF ABBREVIATIONS

PSP	Progressive supranuclear palsy
EIF2AK3	PERK gene
PERK	Protein kinase RNA (PKR)-like endoplasmic reticulum kinase
ER	Endoplasmic reticulum
IRE	Inositol-requiring enzyme 1
ATF6	Activating transcription factor 6
UPR	Unfolded protein response
BiP	Binding immunoglobulin protein
XBP1	X-box binding protein
JNK	C-Jun N-terminal kinase
eIF2α	Alpha subunit of eukaryotic initiation factor 2
ATF4	Activating transcription factor 4
CHOP	CCAAT/enhancer-binding protein (C/EBP) homologous protein
SNP	Single nucleotide polymorphism
TM	Tunicamycin
TG	Thapsigargin
NDC	Non-demented control

LIST OF FIGURES

LIST OF TABLES

ACKNOWLEDGMENTS

Firstly, I would like to acknowledge Dr. Shauna H. S. Yuan for giving me the opportunity to be a part of her lab. She, lab technicians Qing Liu and Patrick C. Reilly, student Kelsey R. Baron, and members of the Wagner Lab Kevin D. Rynearson and Phuong Q. Nguyen have made my first lab experience an unforgettable one.

Next, I would like thank Dr. Maho Niwa Rosen and Dr. Eduardo R. Macagno for being on my thesis committee.

Lastly, I would like to thank post-docs from Dr. Jonathan H. Lin's lab Nobuhiko Hiramatsu and Heike Kroeger for providing me with protocols and reagents for several of my experiments.

ABSTRACT OF THE THESIS

Phenotypic manifestations of EIF2AK3 haplotype B genotypes in fibroblasts derived from patients with progressive supranuclear palsy

by

David Lenh

Master of Science in Biology

University of California, San Diego, 2017

Professor Shauna Hsiao San Yuan, Chair

Professor Maho Niwa Rosen, Co-Chair

Although progressive supranuclear palsy (PSP) is a sporadic neurodegenerative disease, a genome-wide association study identified candidate genes as risk factors. One of these genes EIF2AK3 encodes protein kinase RNA (PKR)-like endoplasmic reticulum kinase (PERK), one of three stress sensors, alongside inositol-requiring enzyme 1 (IRE1) and activating transcription factor 6 (ATF6), in the endoplasmic reticulum (ER). Collectively known as the unfolded protein response (UPR), these sensors attempt to

maintain protein homeostasis before resorting to programmed cell death. IRE1 splices X-box binding protein 1 (XBP1) mRNAs to form transcription factors that upregulate UPR components. ATF6 is modified to form transcription factors that upregulate ER chaperones like binding immunoglobulin protein (BiP). PERK phosphorylates the alpha subunit of eukaryotic initiation factor 2 (eIF2α), attenuating translation with exceptions of activating transcription factor 4 (ATF4) mRNAs. ATF4 then upregulates CCAAT/enhancer-binding protein (C/EBP) homologous protein (CHOP), a proapoptotic protein. Four single nucleotide polymorphisms (SNPs) in PERK are in linkage disequilibrium. The haplotype B variant, with minor alleles for all four, confers deleterious effects. Using patient fibroblasts, this study aimed to characterize the haplotype's effects on PSP pathology and UPR activation. Haplotype B heterozygous fibroblasts displayed heightened sensitivity to ER stress and excessive cell death. Haplotype B fibroblasts had decreased ER stress sensitivity and insignificant amounts of cell death. Basal levels of eIF2α phosphorylation for the two genotypes were comparable. Haplotype B did not affect IRE1 activity and changes in BiP expression, an indicator of ATF6 activation, were drug-dependent only for haplotype B heterozygous fibroblasts.

Introduction

A subset of neurodegenerative diseases is characterized by protein aggregation. In Alzheimer's disease, beta-amyloid, a protein of unknown function, aggregates to form plaques; and tau, a protein that normally binds and stabilizes microtubules, becomes hyperphosphorylated and clusters together to form neurofibrillary tangles.[10] In tauopathies, or neurodegenerative diseases with accumulation of tau protein, aggregated tau no longer upholds the structural integrity of microtubules.[20] Tau accumulation elicits a cellular defense mechanism, the unfolded protein response (UPR), within the endoplasmic reticulum (ER) that attempts to maintain protein homeostasis before resorting to proapoptotic signaling pathways.[1] Although their relationship remains elusive, chronic ER stress and apoptosis due to tauopathies activating the UPR have been linked to neurodegenerative diseases.[13]

Progressive supranuclear palsy (PSP), a lesser known tauopathy, manifests itself with vertical gaze palsy, or the difficulty in moving one's eyes up and down, and symptoms of parkinsonism including rigidity and postural instability.[12] The prevalence of PSP is 6 per 100,000 and the average age of onset is in the early 60's.[9,11] Pathophysiological hallmarks of PSP include neurofibrillary tangles and neurodegeneration in the diencephalon, midbrain, and regions of the hindbrain.[2] Although PSP is a sporadic disease with no known cure, a genome-wide association study revealed candidate genes that contribute to the risk of developing PSP.[7] One of these genes, EIF2AK3, encodes PERK, one of the ER stress sensors in the UPR, and has been linked to neurodegenerative diseases like Alzheimer's disease.[13] This study will attempt to characterize the phenotypes of PERK perturbation and cell death in PSP;

patient-derived fibroblasts will be used to recreate the disease's pathological and genetic information.

In the ER, three transmembrane stress sensors transduce the signal of misfolded proteins and activate downstream pathways that either upregulate chaperone proteins to promote correct folding, halt global translation to alleviate the protein load, or ultimately activate proapoptotic pathways if the UPR fails to maintain proteostasis.[6] BiP, a chaperone protein, normally binds to the stress sensors and keeps them in an inactive state. Once misfolded proteins accumulate in the ER, BiP proteins dissociate from the stress sensors, rendering them active, and bind to misfolded proteins to promote their correct conformation.[19]

One transmembrane stress sensor is an endonuclease/kinase known as IRE1. With the removal of BiP, IRE1 homodimerizes and auto-phosphorylates to become active. With its endonuclease activity, activation of IRE1 results in the splicing of XBP1 mRNAs to form active transcription factors that transcriptionally upregulate ER chaperone genes like BiP.[3] With its kinase activity, IRE1 can also phosphorylate and activate c-Jun N-terminal kinase (JNK), an apoptotic pathway.[17]

Another transmembrane sensor activating transcription factor 6, or ATF6, contains a golgi localization signal that is masked by BiP. The dissociation of BiP from ATF6 leads to its translocation to the golgi where it is then cleaved to form active transcription factors that also transcriptionally upregulates UPR genes.[15]

The third transmembrane stress sensor is PERK (protein kinase RNA (PKR)-like endoplasmic reticulum kinase). Upon activation, PERK phosphorylates its only known substrate the alpha subunit of eIF2, a translation initiation factor, resulting in the

attenuation of global translation with exceptions of ATF4 mRNAs which have upstream open reading frames. ATF4 then upregulates the proapoptotic protein CCAAT/enhancer-binding protein (C/EBP)-homologous protein (CHOP).[4] Further analysis of Hoglinger's genome-wide association study revealed a haplotype variant, or a set of allelic variations that tends to be inherited together, of EIF2AK3 that is associated with increased risk of PSP.[5] The haplotype consists of four single nucleotide polymorphisms (SNPs): one in the intronic region (rs7571971) and three in the coding region of PERK (rs867529, rs13045, rs1805165). The haplotype A variant contains major alleles for the four SNPs, and the haplotype B variant has minor alleles for the four SNPs; major and minor alleles denote protective or risk for the disease, respectively. In addition to the haplotype, there is a rare SNP (rs55791823) also in the coding region (minor allele frequency of 0.016 from screening 84 PSP patients), that is predicted to be damaging.[5]

It is hypothesized that EIF2AK3 haplotype B increases PERK activation, resulting in apoptosis. To investigate the relationship between PERK regulation and cell death, the UPR will be studied in fibroblasts derived from patients diagnosed with PSP and genotyped for the presence of haplotype B. These risk SNPs have been previously shown to upregulate PERK activity, but this disease-in-a-dish model using patient fibroblasts more accurately recreates the pathological genetic and regulatory information.[8] Using non-demented controls (haplotype A) and patient cell lines (haplotype B), and inducing ER stress with either thapsigargin, a sarcoplasmic/endoplasmic reticulum calcium ATPase inhibitor, or tunicamycin, an N-glycosylation inhibitor, different parameters like cell death, eIF2α phosphorylation, CHOP and BiP expression, and XBP1 mRNA splicing will be examined.

Results

SNP genotyping to determine patient genetic profile

Fibroblasts were derived from patients' skin biopsies. Polymerase chain reaction was used to assess whether the cell lines harbored the PERK mutations: genomic DNA was used to sequence the intronic SNP and cDNA, reverse transcribed from RNA, was used to sequence the exonic SNPs. Two non-demented controls (NDC: NDC1, NDC2) did not harbor the intronic SNP (rs7571971), but seven PSP cell lines (IL3, IL8, IL9, FTD38, GIH83, GIH98, GIH99) did. In addition to the rs7571971 SNP, further genotyping revealed that IL3 and IL8 are homozygous for PERK haplotype B (rs867529, rs13045, rs1805165); IL9, FTD38, GIH83, GIH98, and GIH99 are heterozygous for PERK haplotype B. The PSP cell lines were also examined for the presence of rs55791823, a SNP not a part of the haplotype, but still deemed damaging. Only IL3 harbored this SNP (heterozygous). Cell lines NDC1, NDC2, IL3, IL8, IL9, FTD38, GIH83, GIH98, and GIH99 were maintained and expanded for use throughout this project.

Fibroblasts heterozygous for PERK haplotype B are more vulnerable to ER stress exhibiting a cell death phenotype

Using the aforementioned cell lines, cell death was examined using two methods: DAPI staining to quantify nuclear fragmentation, and Western blotting to observe cleaved caspase 3 signals.

Fibroblasts on cover slips were treated with 5μg/mL tunicamycin, and a time course was obtained by fixing and staining with DAPI after 2, 3, and 4 days after treatment. Haplotype A and haplotype B fibroblasts exhibited similar levels of

fragmented nuclei on days 2, 3, and 4. On the other hand, haplotype B heterozygous fibroblasts displayed significantly earlier and more cell death as seen as a twofold, threefold, and fivefold increase in fragmented nuclei on days 2, 3, and 4, respectively (Figure 1A).

After 48 hours of treatment with 5μg/mL tunicamycin, proteins were extracted, and total cell lysates were ran on 12% SDS-PAGE and analyzed by Western blot. When probing for cleaved caspase 3, haplotype A (NDC1) and haplotype B cell lines (IL3 and IL8) did not show signals. The haplotype B heterozygous cell lines IL9 and GIH83 showed two bands, one at 19kDa and another at 17kDa, indicating cleavage of caspase 3, a 36kDa protein (Figure 1B). When increasing the treatment time to 72 hours, another haplotype B heterozygous cell line, FTD38, was also positive for cleaved caspase 3 signals (not shown). In accordance with the nuclear fragmentation, fibroblasts heterozygous for PERK haplotype B were more susceptible to cell death induced by tunicamycin than those that contain haplotype A or haplotype B.

Fibroblasts homozygous and heterozygous for haplotype B display lower basal levels of eIF2α phosphorylation

To evaluate the effects of different PERK haplotype genotypes on PERK activity, basal levels of total eIF2α and phospho-eIF2α were examined by Western blot. Quantifications were performed using ImageLab (BioRad) and eIF2α, phospho-eIF2α, and phospho-eIF2α to total eIF2α ratios were reported. Phospho-eIF2α and total eIF2α levels were comparable for all genotypes (Figure 2). Although not significant, fibroblasts homozygous and heterozygous for haplotype B displayed slightly lower phospho-eIF2α

to total eIF2α ratio levels than haplotype A fibroblasts. Haplotype B did not increase PERK kinase activity, and thus there were no significant changes in phosphorylation of eIF2α.

Fibroblasts heterozygous for PERK haplotype B are more sensitive to ER stress as seen as an increase in CHOP expression levels

To study the different PERK haplotype genotypes' effects on sensitivity to ER stress, fibroblasts were treated with different concentrations of tunicaymin (0.037μg/mL, 0.129μg/mL, 0.454μg/mL, 1.588μg/mL, 5.558μg/mL, 19.453μg/mL) and expression of CHOP mRNA was measured by quantitative real-time polymerase chain reaction (qRT-PCR). Quantification cycle (Cq) values were normalized to an endogenous control RPL19, and then used to calculate average fold change in expression. At a low concentration of 0.129μg/mL, the haplotype B heterozygote (IL9) showed a significant increase in CHOP mRNA levels compared to haplotype A and haplotype B (Figure 3). The effect was more pronounced at a concentration of 0.454μg/mL where CHOP expression was fourfold higher in haplotype B heterozygotes than haplotype A and haplotype B. Comparing haplotype B to haplotype A, the difference in CHOP mRNA levels was not significant, and lower for most of the concentrations used. As seen in the increase in CHOP expression, haplotype B heterozygotes were more sensitive to ER stress than haplotype A and haplotype B.

PERK haplotype B genotypes do not affect IRE1-XBP1 signaling pathway

Fibroblasts were treated with tunicamycin to induce ER stress. cDNA, reverse transcribed from extracted RNA, was used to perform polymerase chain reaction with primers specific to XBP1. XBP1 mRNA splicing was used as a readout for IRE1 activation. The amount of unspliced and spliced XBP1 mRNA was quantified and used to calculate percent splicing (spliced/spliced + unspliced). There was no apparent difference between haplotype A (NDC1, NDC2), haplotype B (IL3, IL8), and haplotype B heterozygotes (IL9) (Figure 4). PERK haplotype genotypes did not affect IRE1 activation, more specifically, XBP1 mRNA splicing.

Crosstalk between PERK and ATF6 is affected by the ER stress inducer used

To examine the crosstalk between PERK and ATF6, ER stress was induced in fibroblasts and changes in BiP mRNA expression were measured by quantitative real-time polymerase chain reaction (qRT-PCR). Once again, RPL19 was used as an endogenous control and quantification cycle (Cq) values were used to calculate average fold change in expression. Thapsigargin and tunicamycin produced differing results. When thapsigargin was used, haplotype B heterozygotes displayed significantly lower levels of BiP expression than haplotype A and haplotype B (Figure 5). However, when tunicamycin was used, haplotype B heterozygotes displayed significantly higher levels of BiP expression than haplotype A and haplotype B.

Table 1. SNP genotyping revealed patient cell lines with different EIF2AK3 haplotype B genotypes. SNP accession number, amino acid, and allele changes are presented. The blue SNPs are in linkage disequilibrium and make up a haplotype. The white SNP (rs55791823) is an extra SNP that is thought to be damaging. Non-demented controls NDC1 and NDC2 did not harbor the intronic SNP rs7571971. IL3, IL8, and GIH99 are homozygous for EIF2AK3 haplotype B; IL9, FTD38, GIH83, and GIH99 are heterozygous for haplotype B. IL3 also harbored rs55791823 (heterozygous) (green = homozygous protective, yellow = heterozygous, red = homozygous risk).

Cell Line	Rs7571971 (intronic) (C/T)	Rs867529 Ser136Cys TCC->TGC (C/G)	Rs13045 Arg166Gln CGA->CAA (G/A)	Rs55791823 Asp566Val GAT->GTT (A/T)	Rs1805165 Ser704Ala TCT->GCT (T/G)
NDC1	C/C				
NDC2	C/C				
IL3	T/T	G/G	A/A	A/T	G/G
IL8	T/T	G/G	A/A	A/A	G/G
IL9	C/T	C/G	G/A	A/A	T/G
FTD38	C/T	C/G	G/A	A/A	T/G
GIH83	C/T	C/G	G/A	A/A	T/G
GIH98	C/T	C/G	G/A	A/A	T/G
GIH99	C/C	G/G	A/A	A/A	G/G

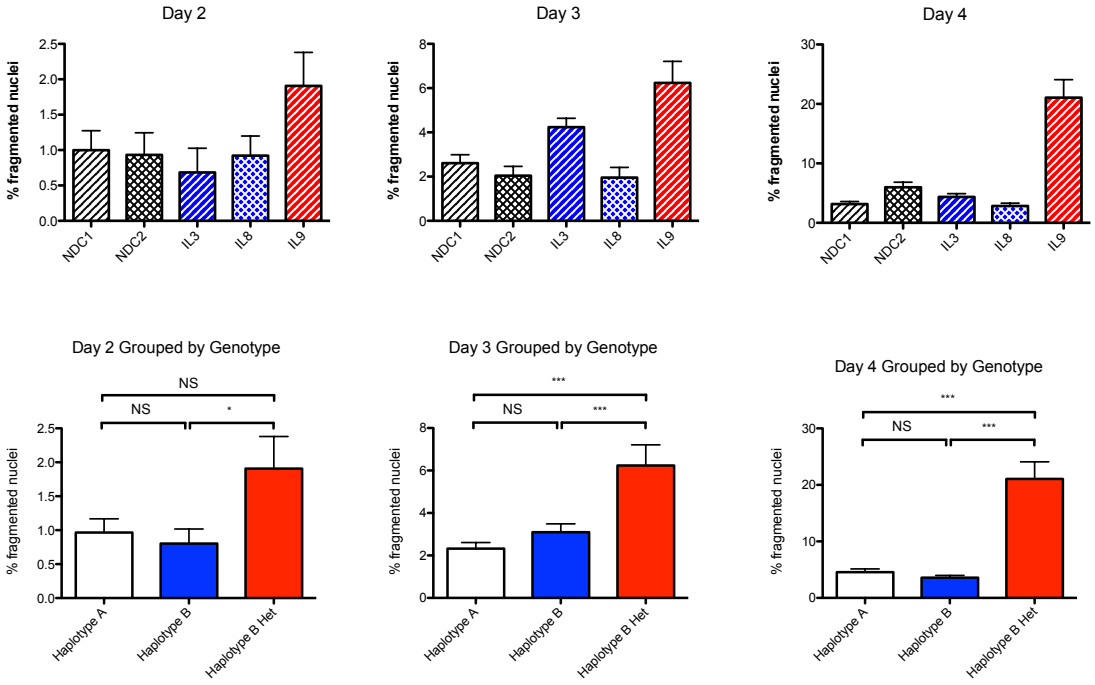

Figure 1A. Fibroblasts heterozygous for haplotype B died sooner and more than other genotypes after treatment with 5µg/mL tunicamycin. Time course of nuclear fragmentation after the indicated amount of days after treatment. The nuclear stain DAPI was used to quantify percent fragmented nuclei (percent of fragmented nuclei was calculated as the number of fragmented nuclei over the total number of nuclei multiplied by 100). Haplotype B heterozygous fibroblasts (in red) died as early as two days after treatment and as much as a fivefold difference four days after treatment. (NS = no significance, * = p-value < 0.05, *** = p-value < 0.001).

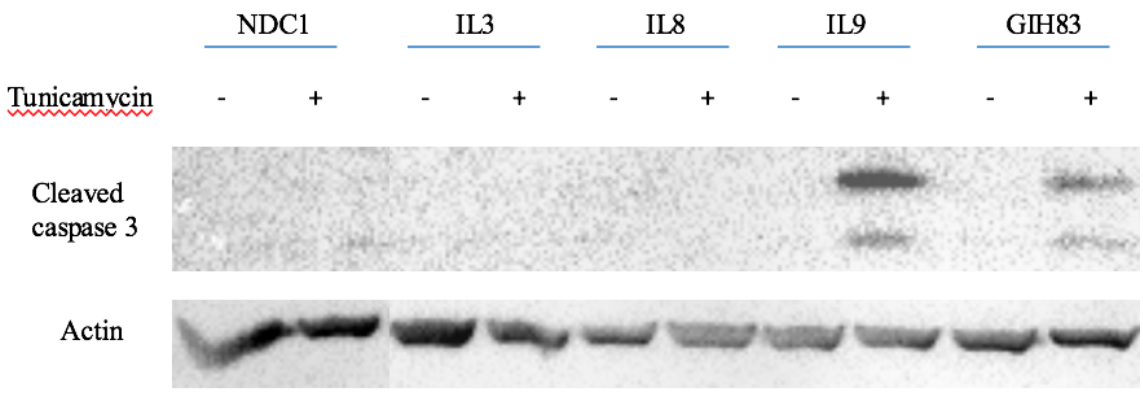

Figure 1B. Fibroblasts heterozygous for haplotype B displayed cleavage of caspase 3 after treatment with 5µg/mL tunicamycin. Cleavage of caspase 3 after 48 hours of treatment with tunicamycin. Haplotype B heterozygous fibroblasts (IL9, GIH83) showed cleavage of caspase 3 into two fragments, indicating apoptosis. Actin was used as a loading control.

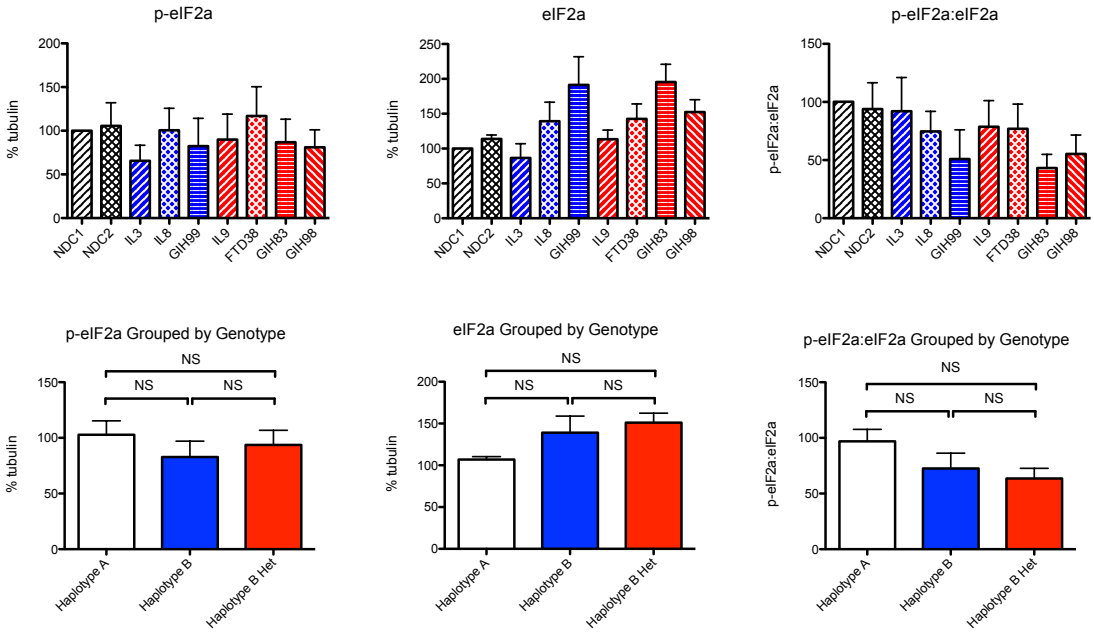

Figure 2. Comparable basal levels of eIF2α phosphorylation in fibroblasts with EIF2AK3 risk SNPs. Densitometric analysis allowed for quantification of eIF2α and phospho-eIF2α based on genotype. Phopho-eIF2α and total eIF2α levels were comparable for all genotypes. When analyzed as the ratio of phospho-eIF2α to total eIF2α, fibroblasts homozygous (in blue) and heterozygous (in red) for haplotype B displayed an insignificantly decreased ratio. (NS = no significance).

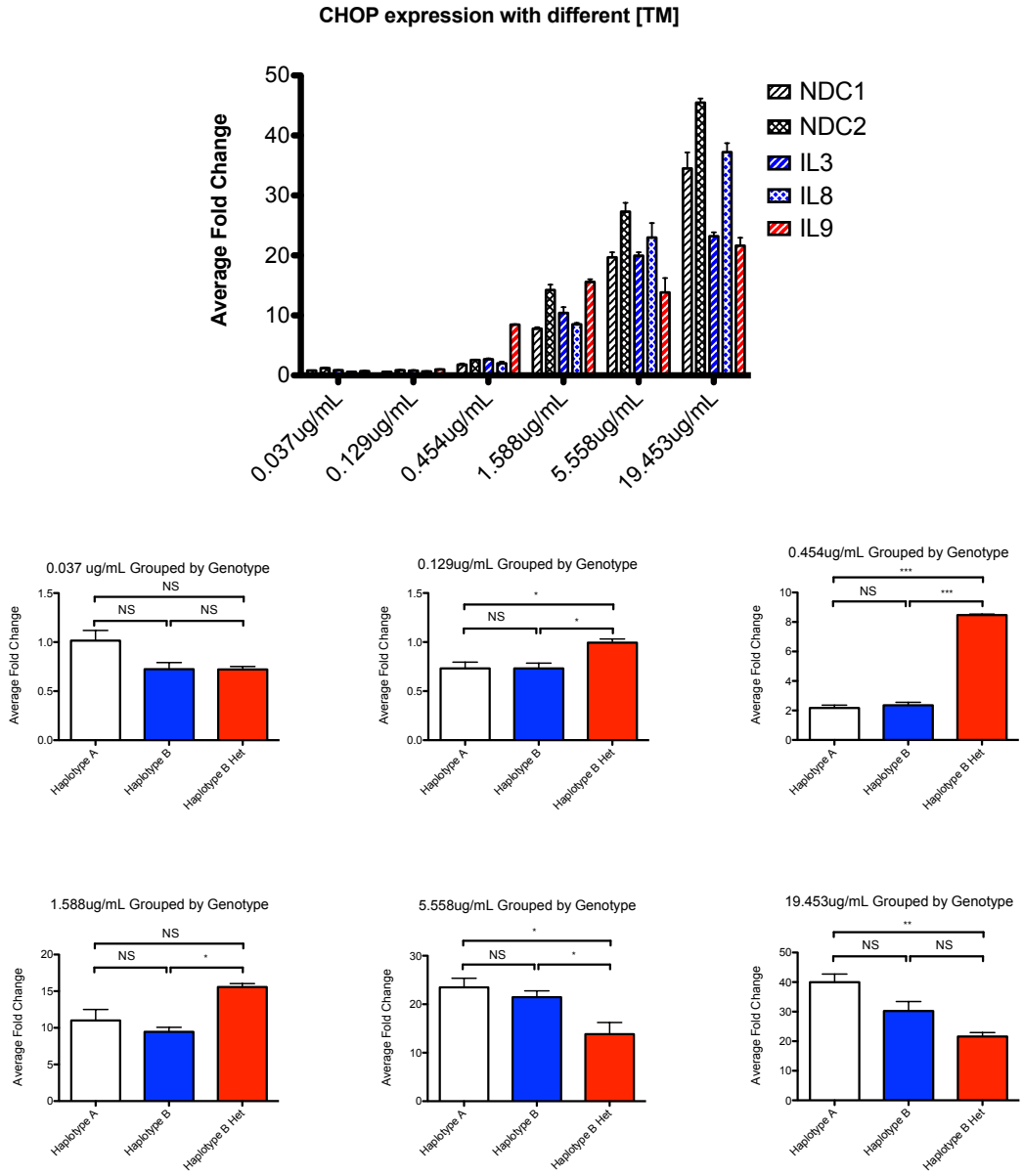

Figure 3. Fibroblasts heterozygous for haplotype B were more vulnerable to ER stress induced by tunicamycin, exhibiting increased CHOP expression levels. Fibroblasts were treated with different concentrations of tunicamycin for 5 hours. Real-time quantitative polymerase chain reaction was used to obtain Cq values. These values were normalized to an endogenous control RPL19 and used to calculate average fold change in CHOP expression. Haplotype B heterozygous (in red) fibroblasts were more sensitive than haplotype A (in white) and haplotype B (in blue) fibroblasts to ER stress as seen in an increase in CHOP expression with as little as 0.129µg/mL tunicamycin. This effect was more pronounced at a concentration of 0.454µg/mL tunicamycin where CHOP expression was fourfold higher for heterozygotes than both haplotype A and B. (NS = no significance, * = p-value < 0.05, ** = p-value < 0.01, *** = p-value < 0.001)

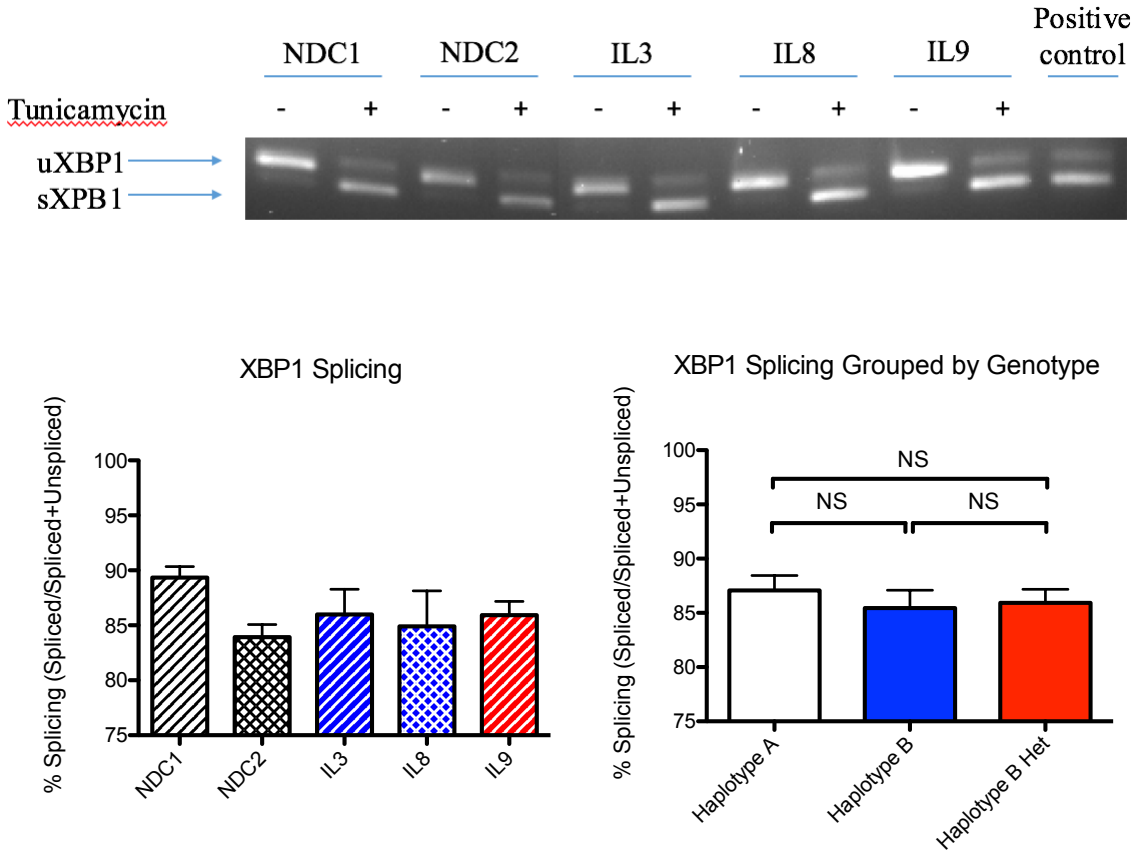

Figure 4. EIF2AK3 haplotype B genotypes did not affect XBP1 splicing. ER stress was induced using 5µg/mL tunicamycin. cDNA, reverse transcribed from RNA, was used to run polymerase chain reaction and amplify XBP1. Amplicons were visualized by 2% agarose gel electrophoresis and densitometric analysis was performed to determine percent splicing (spliced/spliced + unspliced). Spliced XBP1 (sXBP1) contains 26 less nucleotides than unspliced XBP1 (uXBP1) and therefore traveled further down the gel. There were no significant differences in XBP1 splicing for the different haplotype genotypes.

(A)

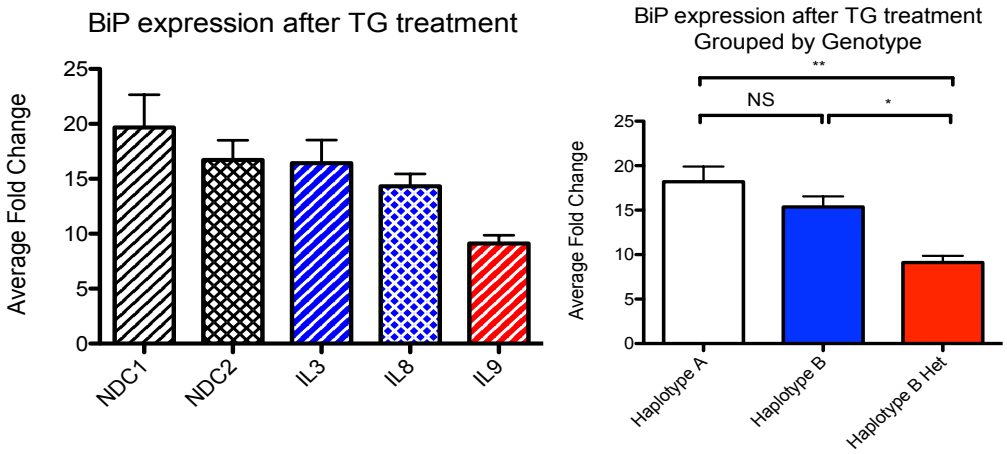

(B)

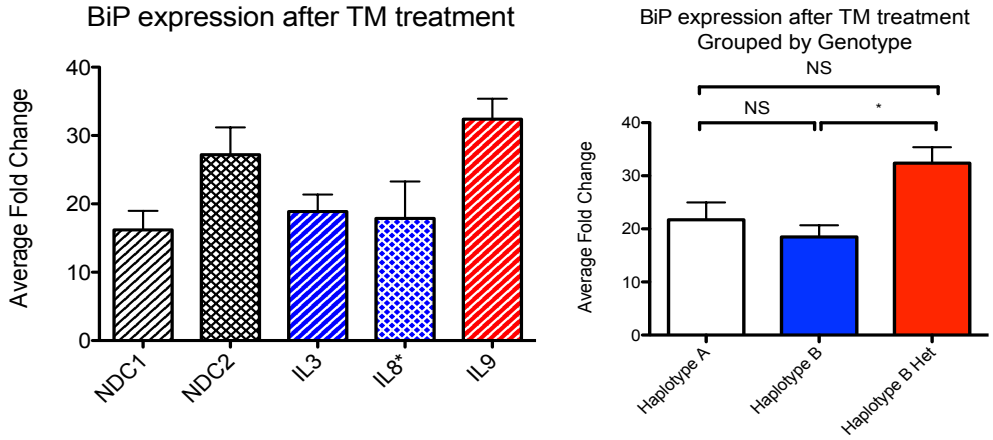

Figure 5. Fibroblasts heterozygous for haplotype B responded differently to thapsigargin and tunicamycin as seen in opposite effects on BiP expression levels. Fibroblasts were treated with either 500nM thapsigargin for 4 hours or 5µg/mL tunicamycin for 5 hours. Real-time quantitative polymerase chain reaction was used to obtain Cq values. These values then were normalized to an endogenous control RPL19 and used to calculate average fold change in BiP expression. Haplotype B (in blue) fibroblasts displayed no significant changes in BiP expression whether thapsigargin or tunicamycin was used. However, haplotype B heterozygous (in red) fibroblasts displayed a decrease in BiP expression in response to thapsigargin (A) and an increase in BiP expression in response to tunicamycin (B). (NS = no significance, * = p-value < 0.05, ** = p-value < 0.01, *** = p-value < 0.001)

Discussion

Due to the heterogeneity from case to case, sporadic diseases are often difficult to study. Genome-wide association studies prove significant in identifying potential genetic factors that contribute to the risk of getting the disease. In addition, a relationship between genotype and phenotype can provide targets for therapeutic advances. This study capitalized on the association of EIF2AK3 single nucleotide polymorphisms (SNPs) and increased risk of getting progressive supranuclear palsy (PSP) to characterize the unfolded protein response (UPR) mechanisms that underlie the disease in patient fibroblasts. This study also profiled the phenotypes associated with a heterozygous variant of the risk haplotype.

EIF2AK3 haplotype B, in which all four SNPs have the minor allele, has been previously linked to neurodegeneration.[13] From the acquired patient fibroblasts, four different genotypes were obtained: controls who do not harbor the EIF2AK3 haplotype SNPs (haplotype A), PSP patients who were heterozygous (haplotype B heterozygous), and homozygous for haplotype B with and without rs55791823. The extra SNP rs55791823 was predicted to be damaging as it affected a conserved residue next to the kinase domain of PERK.[5] The SNP is characterized as the change from the acidic amino acid aspartate at position 566 to valine, a nonpolar amino acid. This nonsynonymous substitution introduces a hydrophobic patch in which chaperone proteins may be recruited for quality control.[18] If the structure is not rescued, PERK's function will be altered; however, IL3, the only cell line with rs55791823 (heterozygous), was no different from other cell lines homozygous for haplotype B in the different parameters observed, indicating the SNP was not damaging as presumed.

The haplotype B heterozygotes should provide insight on the mechanisms behind the pathology because in theory, heterozygotes should have an intermediate phenotype between the protective and risk homozygotes. Unexpectedly, haplotype B cell lines were similar to the haplotype A controls in that they did not show any phenotypes; only haplotype B heterozygous cell lines showed phenotypes of PERK perturbation. If both haplotype B and haplotype B heterozygotes shared similar phenotypes, it is plausible that haplotype B alleles are dominant. However, with some of the parameters in this study, only heterozygous cell lines exhibited phenotypes, indicating that one bad allele is capable of causing the phenotype.

While haplotype B fibroblasts only exhibited cell death comparable to haplotype A, haplotype B heterozygous fibroblasts died as early as two days after treatment and as much as a fivefold difference four days after treatment with tunicamycin (Figure 1A). Consistent with this finding, the heterozygotes, and not haplotype B, were positive for cleaved caspase 3 signals (Figure 1B). Although PERK has been shown to be active in regions where neurodegeneration occurs, haplotype B human fibroblasts did not show signs of apoptosis.[13] The role of PERK haplotype B in inducing cell death may be cell type-dependent whereas neuronal cells are more susceptible than fibroblasts. However, fibroblasts heterozygous for haplotype B displayed excessive cell death and this may be the result of different PERK dimers.

PERK needs to homodimerize in order to become active. In addition to normal homodimers and abnormal homodimers, properly functioning PERK can complex with a malfunctioning monomer to form normal/abnormal heterodimers in haplotype B heterozygous fibroblasts. Fibroblasts homozygous for haplotype B only contain one

PERK dimer conformation: one with two abnormal PERK monomers. The presence of three different PERK dimer complexes found in haplotype B heterozygotes appeared to be more harmful than the abnormal homodimers found in fibroblasts homozygous for haplotype B. The abnormal homodimers with no normally functioning PERK monomer, and not the normal/abnormal heterodimers, may be subjected to ER-associated degradation (ERAD). With the removal of PERK in haplotype B cells, PERK cannot have its downstream effect of apoptosis via CHOP activation. Haplotype B heterozygous cells, similar to haplotype A cells, contain viable PERK dimers that are still able to induce cell death via the eIF2α-ATF4-CHOP pathway; however, haplotype A cells were able to maintain proteostasis without resorting to apoptosis. The mixture of three different PERK dimer complexes may be the cause of unsalvageable ER stress in haplotype B heterozygous fibroblasts; heterozygous PERK knock-ins into either haplotype A or haplotype B cells may reveal the toxicity of different PERK dimers.

EIF2AK3 haplotype B, in which all four SNPs have the minor allele, has been previously linked to increased sensitivity to ER stress in lymphoblastoid cell lines as seen as an increase in eIF2α phosphorylation.[8] However, at basal level, human fibroblasts with haplotype B did not display heightened ER stress sensitivity. Although insignificant, both haplotype B and haplotype B heterozygotes were hypomorphic compared to controls (Figure 2). PERK homodimers and heterodimers arose from different haplotype genotypes, but one bad allele in haplotype B was sufficient in impairing kinase activity, and subsequently decreasing eIF2α phosphorylation.

Continuing examination of the PERK pathway, CHOP expression levels were used as a readout of cell death and ER stress sensitivity of different haplotype genotypes.

In dosage response curves (not shown), fibroblasts homozygous for haplotype B showed a rightward shift, indicating decreased ER stress sensitivity, and fibroblasts heterozygous for haplotype B showed a leftward shift, indicating increased ER stress sensitivity. The heterozygous cells' leftward shift was analogous to a spike in CHOP expression levels in response to a small concentration of tunicamycin (Figure 3) and cell death as seen in fragmented nuclei and cleaved caspase 3 (Figure 1). If haplotype B PERK dimers were degraded via ERAD, there would be no stress sensor present and this can explain the decrease in ER stress sensitivity. Although eIF2α phosphorylation levels were similarly decreased for both genotypes (Figure 2), downstream effectors displayed differing phenotypes.

IRE1 and ATF6 pathways were explored to reveal potential crosstalk and mutated PERK's effect on the other UPR branches. ATF4, which is downstream of the PERK pathway, has been shown to upregulate IRE1α which in turn increases spliced to unspliced ratios of XBP1.[16] Normally with ER stress, IRE1 activation leads to the splicing of XBP1 mRNAs to form active transcription factors that in turn transcriptionally upregulate chaperone genes. Mutated PERK should affect ATF4 translation and ultimately the IRE1-XBP1 signaling pathway. However, haplotype A and haplotype B cell lines, both homozygous and heterozygous, displayed similar amounts of spliced XBP1 mRNA at around 85% splicing (Figure 4). Although ATF4 was not directly measured, basal levels of eIF2α phosphorylation, which is upstream of ATF4, were used to predict changes in ATF4 levels. Since eIF2α phosphorylation levels were similarly hypomorphic in all haplotype genotypes, ATF4 was not particularly upregulated, and thus XBP1 splicing was affected to a similar extent. Transcriptional analysis of ATF4

levels can be used to verify its effect on XBP1 splicing. In conclusion, PERK mutations did not affect IRE1's endonuclease activity.

Normally with ER stress, ATF6 translocates to the golgi where it is cleaved to form active transcription factors. BiP is then transcriptionally upregulated to increase ER protein folding capacity. ATF4 has been shown to enhance the transcription of the ATF6 gene and contribute to the trafficking of ATF6 from the ER to the golgi.[14] PERK mutations that alter ATF4 should also hinder ATF6 transcription, translocation, and ultimately BiP expression. Basal levels of eIF2α phosphorylation were once again used to predict changes in ATF4 levels: with both haplotype B genotypes, homozygous and heterozygous, displaying hypomorphic levels of basal eIF2α phosphorylation, ATF4 should not be particularly upregulated. Haplotype A and haplotype B had comparable BiP expression for both thapsigargin and tunicamycin; however, haplotype B heterozygotes had differing results depending on the drug used to induce ER stress. Tunicamycin, which prevents the posttranslational modification of N-glycosylation, had the expected result of increasing BiP expression. Unexpectedly, thapsigargin, a sarcoplasmic/endoplasmic reticulum calcium ATPase inhibitor that depletes calcium in the ER, decreased BiP expression. BiP expression was expected to increase, but the change in calcium levels induced by thapsigargin, and not the lack of posttranslational modifications elicited by tunicamycin may have caused the mixture of PERK dimers, products of haplotype B heterozygosity, to respond differently and result in opposite effects on BiP expression. BiP expression may have been diminished, but a follow-up experiment evaluating BiP protein levels may provide insight on the ER's protein folding capacity in response to thapsigargin.

Fibroblasts derived from patients diagnosed with PSP allowed for genotypic profiling and characterization of UPR phenotypic manifestations. Although this model allows for the preservation of the disease's genetic and pathological components, fibroblasts, which lack tau, are not the cells of primary interest; neuronal cells, which include tau, are a more representative model when studying neurodegenerative diseases like tauopathies. In addition to contributing to current literature with PERK haplotype A and haplotype B phenotypes, this study starts the discussion of PERK haplotype B heterozygosity: data gathered from fibroblast have shown haplotype B heterozygosity rather than homozygosity to be deleterious. Cell type dependence might have been a factor as to why haplotype B fibroblasts did not exhibit cell death. Future studies with neuronal cultures derived from patients will further elucidate the role of PERK haplotype B and the UPR on neurodegeneration in PSP.

Materials and Methods

Media composition and maintenance of primary fibroblast culture

Primary fibroblast media: Dulbecco's Modified Eagle Medium (DMEM, high glucose; Life Technologies) supplemented with 15% FBS, 2mM L-glutamine (Life Technologies), 0.1mM MEM nonessential amino acids (Life Technologies), 1X penicillin-streptomycin (pen-strep; Life Technologies), and 1mM sodium pyruvate (Life Technologies). Adult human dermal fibroblasts were manually passaged onto 0.1% porcine gelatin (Sigma-Aldrich) coated plates. Treatments included tunicamycin (Sigma-Aldrich) with dimethylformamide (DMF) as the vehicle and thapsigargsin (Sigma-Aldrich) with dimethyl sulfoxide (DMSO) as the vehicle. Cells were washed with Dulbecco's Phosphate-Buffered Saline (DPBS; Life Technologies), trypsinized with 0.05% trypsin (Life Technologies), washed again with DPBS, and then centrifuged to form pellets. The cell pellets were stored at -80C until genomic DNA, RNA, or protein extraction.

RNA extraction and cDNA preparation

The RNeasy™ Mini Kit (Qiagen) was used to extract total RNA from the cell pellets. The iScript™ cDNA Synthesis Kit (BioRad) was used to reverse transcribe total RNA into cDNA. 5X reaction mix, iScript reverse transcriptase, 1µg of RNA template, and water were combined for a total reaction volume of 20µL. The reactions were incubated for 5 min at 25C, 30 min at 42C, and 5 min at 85C. The cDNA samples were stored at -20C until amplification using PCR or transcriptional analysis using qPCR.

Sequencing using polymerase chain reaction (PCR)

Genomic DNA, used to sequence the intronic SNP (rs7571971), was extracted from fibroblast cell pellets using the Quick-gDNA™ MiniPrep Kit (Zymo Research). The primers used are listed in Table 2.

A 620 bp fragment containing the SNPs rs867529 and rs13045, and a 418 bp fragment containing the SNP rs1805165 were amplified from cDNA using Phusion® High-Fidelity DNA Polymerase. A 640 bp fragment containing the SNP rs55791823 was amplified from cDNA using PicoMaxx High Fidelity PCR System.

For the Phusion® protocol, 1.5µg of cDNA template, 10µM of each primer, 5X HF buffer, 100mM dNTPs, Phusion® polymerase, and water were combined for a total reaction volume of 20µL. The cycle conditions were 30 sec at 98C, 30 cycles with 10 sec denaturation at 98C, 30 sec annealing at 50C, 30 sec elongation at 72C, and 30 sec at 72C.

For the PicoMaxx protocol, 3µg of cDNA template, 10µM of each primer, 10X reaction buffer, 100mM dNTP, PicoMaxx polymerase, and water were combined for a total reaction volume of 25µL. The cycle conditions were 2 min at 95C, 35 cycles with 40 sec denaturation at 95C, 30 sec annealing at 50C, 1 min elongation at 72C, and 10 min at 72C.

Samples were mixed with 6X Orange G loading dye and visualized by 1% agarose gel electrophoresis. Bands were excised and purified using the Zymoclean™ Gel DNA Recovery Kit. Purified PCR products were then submitted with the appropriate primers for Sanger sequencing (Eton Bioscience, San Diego, CA, USA).

Table 2. List of primers used for genotyping PERK SNPs.

Target SNP(s)	Primer	Sequence (5' – 3')	Product Size (bp)
rs7571971	Forward	TCTCCCAGAAAAATAGAAGCATCATACC	223
	Reverse	GACCCTTTTGGCCCATGGTAAA	
rs867529, rs13045	Forward	ACGCTGATGGAGCGCGCCAT	620
	Reverse	CTGAGTCCATATGTAGTCAG	
rs1805165	Forward	GAATTGGCTCGGGAAAAGGT	418
	Reverse	AGTCTGTAAGGCAACTGTCCTG	
rs55791823	Forward	ATGTATAGAGGCCAGCTGTA	640
	Reverse	CACCACGTCCCAGGCATTGA	

DAPI staining

Fibroblasts were plated at a concentration of 50,000 cells/well onto gelatin-coated coverslips in 24-well plates. Cells were treated with 5µg/mL tunicamycin and DMF was used as a vehicle; treatment was performed in duplicates. After 2, 3, and 4 days of treatment, cells were washed twice with DPBS, fixed with 4% paraformaldehyde, washed thrice with DPBS, blocked with 4% bovine serum albumin (BSA; Sigma-Aldrich), and stained with DAPI 1:1000 in DPSB. After the coverslips were mounted onto slides, five 10X images were taken for each coverslip. The percent of fragmented nuclei was calculated as the number of fragmented nuclei over the total of total number of nuclei multiplied by 100.

Protein preparation and western blotting

RIPA lysis buffer was prepared with 50mM Tris (pH 7.4), 150mM NaCl, 1% Triton X-100, 1mM EDTA (pH 7.5), 0.1% SDS, 0.25% Na-deoxycholate, 1mM EGTA, 100X protease and phosphatase inhibitors. Cell pellets were incubated in RIPA lysis buffer on ice for 30 min and vortexed every 10 min. Cell lysates were collected after centrifuging for 20 min. Fifteen to twenty micrograms of total cell lysate were loaded onto SDS-PAGE mini gels and analyzed by Western blot.

The following primary antibodies and dilutions were used: anti-eIF2α (Abcam, *ab26197*, 1:4000), anti-phospho-eIF2α (Abcam, *ab32157*, 1:4000), anti-cleaved caspase 3 (Cell Signaling Technology, *ab9661*, 1:1000), anti-tubulin (Sigma-Aldrich, *T5293*, 1:16000), anti-actin (Sigma-Aldrich, *A5316*, 1:8000). After overnight incubation with the primary antibody, membranes were washed in Tris-Buffered Saline (TBS) containing

0.1% Tween-20 (Sigma-Aldrich) and incubated in horseradish peroxidase (HRP)-coupled secondary antibody (diluted 1:4000 in 5% nonfat dry milk in 1X TBST. Immunoreactivity was detected using Clarity™ Western ECL Substrates (BioRad).

qRT-PCR transciptional analysis of CHOP and BiP

Twenty nanograms of cDNA were used in qPCR analysis using iQ™ SYBR® Green Supermix (BioRad). Reactions were performed in triplicates. The cycle conditions were 5min at 95C, 40 cycles with 10 sec denaturation at 95C, 10 sec annealing at 58C, 10 sec at 72C. Melt curves were ran in 10 sec increments from 45C to 95C. Average fold change in expression was reported using Cq values.

RT-PCR for the detection of XBP1 splicing

Five hundred micrograms of cDNA were used to amplify XBP1. The primers used are listed in Table 3. The cycle conditions were 3 min at 94C, 35 cycles with 30 sec denaturation at 94C, 30 sec annealing at 58C, 30 sec elongation at 72, and 5 min at 72C. Samples were mixed with 6X Orange G loading dye and visualized by 2% agarose gel electrophoresis. Amplicons were ran for 70 minutes at 100V for good separation. Densitometric analysis was performed using ImageLab (BioRad) to determine percent splicing of XBP1 (spliced/spliced + unspliced).

Table 3. List of primers used for transcriptional analysis of CHOP and BiP, and detection of XBP1 splicing.

Target Gene	Primer	Sequence (5' – 3')	Product Size (bp)
CHOP	Forward	ACCAAGGGAGAACCAGGAAACG	201
	Reverse	TCACCATTCGGTCAATCAGAGC	
RPL19	Forward	ATGTATCACAGCCTGTACCTG	233
	Reverse	TTCTTGGTCTCTTCCTCCTTG	
BiP	Forward	CGGGCAAAGATGTCAGGAAAG	221
	Reverse	TTCTGGACGGGCTTCATAGTAGAC	
XBP1	Forward	TTACGAGAGAAAACTCATGGC	Unspliced – 283 Spliced – 257
	Reverse	GGGTCCAAGTTGTCCAGAATGC	

References

1. Abisambra, J. F., Jinwal, U. K., Blair, L. J., O'leary, J. C., Li, Q., Brady, S., Wang, L., Guidi, C. E., Zhang, B., Nordhues, B. A., Cockman, M., Suntharalingham, A., Li, P., Jin, Y., Atkins, C. A. And Dickey, C. A. 2013. Tau Accumulation Activates the Unfolded Protein Response by Impairing Endoplasmic Reticulum-Associated Degradation. Journal of Neuroscience 33:9498-9507.

2. Boxer, A. L., Geschwind, M. D., Belfor, N., Gorno-Tempini, M. L., Schauer, G. F., Miller, B. L., Weiner, M. W. And Rosen, H. J. 2006. Patterns of Brain Atrophy That Differentiate Corticobasal Degeneration Syndrome From Progressive Supranuclear Palsy. Archives of Neurology 63:81.

3. Calfon, M., Zeng, H., Urano, F., Till, J. H., Hubbard, S. R., Harding, H. P., Clark, S. G. And Ron, D. 2002. IRE1 couples endoplasmic reticulum load to secretory capacity by processing the XBP-1 mRNA. Nature 415:92-96.

4. Chakrabarti, A., Chen, A. W. And Varner, J. D. 2011. A review of the mammalian unfolded protein response. Biotechnology and Bioengineering 108:2777-2793.

5. Ferrari, R., Ryten, M., Simone, R., Trabzuni, D., Nicolaou, N., Hondhamuni, G., Ramasamy, A., Vandrovcova, J., Weale, M. E., Lees, A. J., Momeni, P., Hardy, J. And De Silva, R. 2014. Assessment of common variability and expression quantitative trait loci for genome-wide associations for progressive supranuclear palsy. Neurobiology of Aging 35:1514.e1-1514.e12.

6. Hetz C. 2012. The unfolded protein response: controlling cell fate decisions under ER stress and beyond. Nature Reviews Molecular Cell Biology.

7. Höglinger, G. U., Melhem, N. M., Dickson, D. W., Sleiman, P. M. A., Wang, L., Klei, L., Rademakers, R., De Silva, R., Litvan, I., Riley, D. E., Van Swieten, J. C., Heutink, P., Wszolek, Z. K., Uitti, R. J., Vandrovcova, J., Hurtig, H. I., Gross, R. G., Maetzler, W., Goldwurm, S., Tolosa, E., Borroni, B., Pastor, P., Albin, R. L., Alonso, E., Antonini, A., Apfelbacher, M., Arnold, S. E., Avila, J., Beach, T. G., Beecher, S., Berg, D., Bird, T. D., Bogdanovic, N., Boon, A. J. W., Bordelon, Y., Brice, A., Budka, H., Canesi, M., Chiu, W. Z., Cilia, R., Colosimo, C., De Deyn, P. P., De Yebenes, J. G., Kaat, L. D., Duara, R., Durr, A., Engelborghs, S., Fabbrini, G., Finch, N. A., Flook, R., Frosch, M. P., Gaig, C., Galasko, D. R., Gasser, T., Gearing, M., Geller, E. T., Ghetti, B., Graff-Radford, N. R.,

Grossman, M., Hall, D. A., Hazrati, L., Höllerhage, M., Jankovic, J., Juncos, J. L., Karydas, A., Kretzschmar, H. A., Leber, I., Lee, V. M., Lieberman, A. P., Lyons, K. E., Mariani, C., Masliah, E., Massey, L. A., Mclean, C. A., Meucci, N., Miller, B. L., Mollenhauer, B., Möller, J. C., Morris, H. R., Morris, C., O'sullivan, S. S., Oertel, W. H., Ottaviani, D., Padovani, A., Pahwa, R., Pezzoli, G., Pickering-Brown, S., Poewe, W., Rabano, A., Rajput, A., Reich, S. G., Respondek, G., Roeber, S., Rohrer, J. D., Ross, O. A., Rossor, M. N., Sacilotto, G., Seeley, W. W., Seppi, K., Silveira-Moriyama, L., Spina, S., Srulijes, K., St. George-Hyslop, P., Stamelou, M., Standaert, D. G., Tesei, S., Tourtellotte, W. W., Trenkwalder, C., Troakes, C., Trojanowski, J. Q., Troncoso, J. C., Van Deerlin, V. M., Vonsattel, J. P. G., Wenning, G. K., White, C. L., Winter, P., Zarow, C., Zecchinelli, A. L., Cantwell, L. B., Han, M. R., Dillman, A., Van Der Brug, M. P., Gibbs, J. R., Cookson, M. R., Hernandez, D. G., Singleton, A. B., Farrer, M. J., Yu, C., Golbe, L. I., Revesz, T., Hardy, J., Lees, A. J., Devlin, B., Hakonarson, H., Müller, U. And Schellenberg, G. D. 2011. Identification of common variants influencing risk of the tauopathy progressive supranuclear palsy. Nature Genetics 43:699-705.

8. Liu, J., Hoppman, N., O'connell, J. R., Wang, H., Streeten, E. A., Mclenithan, J. C., Mitchell, B. D. And Shuldiner, A. R. 2012. A functional haplotype in EIF2AK3, an ER stress sensor, is associated with lower bone mineral density. Journal of Bone and Mineral Research 27:331-341.

9. Maher, E. R. And Lees, A. J. 1986. The clinical features and natural history of the Steele-Richardson-Olszewski syndrome (progressive supranuclear palsy). Neurology 36:1005-1005.

10. Mandelkow EM, Mandelkow E. 1998. Tau in Alzheimer's disease. Trends Cell Biology 8:425–427.

11. Schrag, A., Ben-Shlomo, Y. And Quinn, N. 1999. Prevalence of progressive supranuclear palsy and multiple system atrophy: a cross-sectional study. The Lancet 354:1771-1775.

12. Steele, J. C. 1964. Progressive Supranuclear Palsy. Archives of Neurology 10:333.

13. Stutzbach, L. D., Xie, S. X., Naj, A. C., Albin, R., Gilman, S., Lee, V. M. Y., Trojanowski, J. Q., Devlin, B. And Schellenberg, G. D. 2013. The unfolded

protein response is activated in disease-affected brain regions in progressive supranuclear palsy and Alzheimer's disease. Acta Neuropathologica Communications 1:31.

14. Teske, B. F., Wek, S. A., Bunpo, P., Cundiff, J. K., Mcclintick, J. N., Anthony, T. G. And Wek, R. C. 2011. The eIF2 kinase PERK and the integrated stress response facilitate activation of ATF6 during endoplasmic reticulum stress. Molecular Biology of the Cell 22:4390-4405.

15. Todd, D. J., Lee, A. And Glimcher, L. H. 2008. The endoplasmic reticulum stress response in immunity and autoimmunity. Nature Reviews Immunology 8:663-674.

16. Tsuru, A., Imai, Y., Saito, M. And Kohno, K. 2016. Novel mechanism of enhancing IRE1α-XBP1 signalling via the PERK-ATF4 pathway. Scientific Reports 6.

17. Urano F. 2000. Coupling of Stress in the ER to Activation of JNK Protein Kinases by Transmembrane Protein Kinase IRE1. Science 287:664-666.

18. Vembar, S. S. And Brodsky, J. L. 2008. One step at a time: endoplasmic reticulum-associated degradation. Nature Reviews Molecular Cell Biology 9:944-957.

19. Wang, M., Wey, S., Zhang, Y., Ye, R. And Lee, A. S. 2009. Role of the Unfolded Protein Response Regulator GRP78/BiP in Development, Cancer, and Neurological Disorders. Antioxidants & Redox Signaling 11:2307-2316.

20. Williams, D. R. 2006. Tauopathies: classification and clinical update on neurodegenerative diseases associated with microtubule-associated protein tau. Internal Medicine Journal 36:652-660.